Effect of Water Adsorption on Retention of Structure and Surface Area of Metal–Organic Frameworks

ARTICLE *in* INDUSTRIAL & ENGINEERING CHEMISTRY RESEARCH · APRIL 2012

Impact Factor: 2.59 · DOI: 10.1021/ie202325p

5 AUTHORS, INCLUDING:

Cantwell Carson
National Energy Technology Laboratory
18 PUBLICATIONS **399** CITATIONS

SEE PROFILE

Himanshu Jasuja
Georgia Institute of Technology
16 PUBLICATIONS **471** CITATIONS

SEE PROFILE

I&EC research
Industrial & Engineering Chemistry Research

Article

pubs.acs.org/IECR

Effect of Water Adsorption on Retention of Structure and Surface Area of Metal−Organic Frameworks

Paul M. Schoenecker, Cantwell G. Carson, Himanshu Jasuja, Christine J. J. Flemming, and Krista S. Walton*

School of Chemical and Biomolecular Engineering, Georgia Institute of Technology, 311 Ferst Drive NW, Atlanta, Georgia 30332, United States

Supporting Information

ABSTRACT: This work presents an experimental investigation of water adsorption in metal−organic frameworks (MOFs) at room temperature and up to 90% relative humidity. Structural degradation of the materials after regeneration is analyzed via powder X-ray diffraction (PXRD) and nitrogen adsorption measurements. MOFs with open metal sites are quite hydrophilic but appear to maintain their structure according to PXRD. However, significant surface area loss indicates that decomposition is occurring and is likely an attribute of oxygen presence during the regeneration procedure. Materials with copper paddle-wheel (HKUST-1), 5-coordinated magnesium (Mg MOF-74), and 7-coordinated zirconium (UiO-66(-NH_2)) maintain good structural stability, while Zn-COOH containing MOFs (DMOF-1; DMOF-1-NH_2; UMCM-1) undergo complete loss of crystallinity.

1. INTRODUCTION

The ability to synthesize metal−organic frameworks (MOFs) with prescribed structural features has led to intense interest in the materials for selective adsorption processes. The hybrid nature of MOFs provides an almost infinite set of building blocks that can be manipulated to target specific adsorption behavior by introducing open metal sites and functional groups, or by further modulating the properties by postsynthetic modification.[1−8] To date, much of the experimental and theoretical research on MOF applications has centered on adsorption simulations and measurements. Investigations of gas storage (hydrogen/methane) and carbon dioxide capture from flue gas have been a particular focus.[2,3,8]

Aside from good adsorption loadings and high selectivities, the stability of an adsorbent in humid environments is a critical property that must be considered when designing an adsorption process. The water sensitivity of certain MOFs has been well-documented,[9−13] but a variety of MOFs including pyrazolate[14] and imidazolate[15] frameworks and zirconium-based MOFs[16] have been reported in recent years that do not lose structural integrity in the presence of water. Long and co-workers have reported pyrazolate-based MOFs that show remarkable structural integrity after exposure to boiling water and other solvents due to the high pK_a value of the ligands. These materials also possess open metal sites.[14] Lillerud and co-workers have reported an interesting family of isoreticular zirconium MOFs built from various aromatic carboxylates.[16] UiO-66 shows no change in PXRD pattern after exposure to liquid water and other solvents. The stability is attributed to the strength of the inorganic unit; each zirconium atom is 8-coordinated via terephthalic acid ligands. Several MIL materials are known to maintain good structural integrity after water exposure due to high coordination numbers,[17−19] and the zeolitic imidazolate frameworks (ZIFs) have also shown good stability under aqueous conditions.[15,19]

Cychosz and Matzger[20] recently reported an investigation of the stability of several MOFs after exposure to aqueous solutions with varying amounts of DMF. MOF structures utilizing Zn-carboxylate connectivity (MOF-5, MOF-177) were found to be unstable after exposure to liquid water, while copper paddle-wheel MOFs (HKUST-1, MOF-505) showed good structure retention after similar testing. An investigation by Low et al.[21] using high throughput steam treatment found that metal−ligand bond strength and oxidation state of the metal cluster are important contributors to MOFs stability. Kaskel et al.[19] reported water adsorption isotherms for several MOFs; HKUST-1, ZIF-8, DUT-4, MIL-100, and MIL-101. Water stability was analyzed following the water vapor adsorption as well as after immersing the MOFs in liquid water at 323 K. The Dietzel group has investigated the stability of the MOF-74/CPO-27 materials (Co, Mg, Ni) throughout dehydration/rehydration cycling.[22−24] The MOF-74 analogues were found to be stable during cyclic adsorption testing while using inert gases (Ar/N_2). However, when the same experiment was conducted in air, the Ni MOF-74 degraded.[23]

Sensitivity to water vapor is widely considered to be a major weakness of MOFs that could negate potential advantages of the hybrid materials from an applications perspective. Understanding the behavior of MOFs under humid conditions is quite important for applications such as CO_2 capture from flue gas or air purification. The importance of MOF performance in humid environments cannot be overstated, and understanding the parameters that contribute to this sensitivity is critical for elevating MOFs to the applied level. Nevertheless, few systematic studies on the stability of MOFs after exposure to humid streams have been reported. In this work, we present an

Received: October 12, 2011
Revised: March 12, 2012
Accepted: March 28, 2012
Published: March 28, 2012

dx.doi.org/10.1021/ie202325p | *Ind. Eng. Chem. Res.* 2012, 51, 6513−6519

experimental investigation of water adsorption in MOFs at room temperature and up to 90% relative humidity (RH), followed by an analysis of structural degradation and surface area change. Specifically, we examine structure retention after water exposure and regeneration via dynamic vacuum and elevated temperature, due to the direct link with many gas separation applications.

Seven MOFs were selected for this study to represent a range of features that are common in MOFs. These include open-metal sites (HKUST-1,[25] Mg-MOF-74[26]), amine-functional groups (UiO-66,[27] DMOF-1[5,28]), carboxylate coordination (UMCM-1,[29] HKUST-1, Mg-MOF-74), and nitrogen coordination (DMOF-1). There are also differences in the metal coordination as these MOFs are synthesized from zinc, copper, magnesium, or zirconium. The isoreticular family of UiO-66 materials also contain open-metal sites upon activation or dehydroxylation.[16,30,31] However, Llewellyn et al.[32] shows that these open Zr sites do not interact with gases like CO and CO_2 in the same fashion as other open-metal site MOFs, e.g., HKUST-1. So, UiO-66 and UiO-66-NH_2 are not considered in the same category as Mg-MOF-74 and HKUST-1 for this study.

HKUST-1, or Cu-BTC, is one of the most widely studied MOFs over the past decade.[19,33−36] This material is synthesized from a mixture of $Cu(NO_3)_2{\cdot}3H_2O$ and 1,3,5-benzene tricarboxylic acid (BTC) in deionized water and ethanol. The secondary building unit is formed by the copper paddlewheel, in which Cu−Cu dimers are connected by BTC ligands. The large pore diameter is 9 Å, and the small pores are around 6 Å. An open coordination site is generated at each copper upon activation of the material. Wang et al.[36] reported the first water isotherm for HKUST-1, but no structure or surface area analyses were performed. Low et al.[21] reported that HKUST-1 is stable up to 200 °C when exposed to 50 mol % steam, and Cychosz and Matzger[20] found that HKUST-1 exhibits good structure retention in a 7:1 mixture of H_2O:DMF even after 21 months of exposure. In contrast, Kaskel et al.[19] determined from powder X-ray diffraction that HKUST-1 breaks down after immersion in pure water at 323 K for 24 h.

Mg-MOF-74 is synthesized from magnesium and 2,5-dihydroxyterephthalic acid. It possesses one-dimensional channels of approximately 11 Å diameter in a honeycomb topology, with removable solvent molecules coordinating at the metal sites. Of the open-metal site MOFs, Mg MOF-74 exhibits among the highest loadings of CO_2 at low pressure (e.g., 35.2 wt % uptake of CO_2 at 298 K and 1 atm).[3] It also has been reported to exhibit a strong affinity for water,[34,36,38] but the effect of water adsorption and regeneration on available surface area has not been investigated.

UiO-66 contains $[Zr_6O_4(OH)_4]$ clusters linked with twelve terephthalate moieties. The pore diameters are approximately 6 Å. Upon dehydroxylation $[Zr_6O_4(OH)_4]$ clusters change to $[Zr_6O_6]$, and the Zr metal-centers undergo a transition from the as-synthesized 8-coordinated state to 7-coordinated state.[31] Previous studies have shown that UiO-66 maintains its structure after immersion in water and other solvents, but no water isotherms were reported.[16]

Nitrogen-coordinated DMOF-1 ($Zn_2(BDC)_2(DABCO)$) has square-shaped channels of 7.5 Å diameter that are interconnected by smaller pores with diameters of 4.8 × 3.2 Å. It has been shown to be hydrophobic up to 42% RH, but no structure analysis was performed postexposure.[28] On the other hand, Liang et al.[38] investigated the water tolerance of zinc and nickel versions of this material and found that both appear to lose structural integrity after exposure to relative humidity above 60%. The corresponding surface area analysis was not performed.

MOFs with amine-functionalized ligands often provide the functional sites capable of facilitating postsynthetic modification (PSM),[7,39] and therefore, are of great importance when considering PSM materials for humid gas separation processes. There have been no water adsorption or stability studies reported for the amine containing analogues, UiO-66-NH_2 and DMOF-1-NH_2.

UMCM-1 is a mesoporous MOF synthesized from zinc and two organic ligands, terephthalic acid and 1,3,5-tris(4-carboxyphenyl)benzene (BTB). This MOF has shown some promise for dry gas separation applications.[40] However, with a coordination environment similar to MOF-5, it is unlikely that UMCM-1 will exhibit great water stability.

2. EXPERIMENTAL SECTION

2.1. Synthesis Methods. All chemicals were procured from commercial sources (Fisher and Sigma Aldrich) and used without further purification. Samples were stored in sealed vials prior to use.

UMCM-1. A modified version of the previously reported synthesis method[29] was used. $Zn(NO_3)_2{\cdot}6H_2O$ (3.87 g, 13.0 mmol), terephthalic acid (TPA) (0.540 g, 3.25 mmol), and 1,3,5-tris (carboxyphenyl) benzene (1.28 g, 2.92 mmol) were dissolved in 120 mL of diethylformamide (DEF). The solution was then filtered twice to remove undissolved solids and divided into twelve 20 mL scintillation vials in a sand bath. The sand bath was heated to 85 °C for 48 h. The product was rinsed with dimethylformamide (DMF) three times before solvent exchanging with dichloromethane (CH_2Cl_2) for 96 h via Sohxlet extraction prior to activation at 150 °C.

Mg MOF-74. The reported synthesis method[3] was implemented as follows: $Mg(NO_3)_2{\cdot}6H_2O$ (1.90 g, 7.4 mmol) and 2,5-dioxido-1,4-benzenedicarboxylic acid (H_4DOBDC) (0.444 g, 7.40 mmol) were placed in a 200 mL of DMF:ethanol:water (15:1:1, by volume). The resultant mixture was sonicated until homogeneous. Then, 10 mL portions of the solution were placed in 20 mL scintillation vials and placed in a sand bath. The sand bath was heated to 125 °C, and the solution was allowed to react for 20 h. The resultant product was collected and placed in a Sohxlet extractor for 96 h to exchange with methanol before activation at 250 °C.

HKUST-1. HKUST-1 was synthesized as follows: $Cu(NO_3)_2{\cdot}3H_2O$ (4.55 g, 18.8 mmol) was dissolved in 60 mL of deionized water and trimesic acid (2.10 g, 9.99 mmol) was dissolved in 60 mL of ethanol via sonication. The solutions were added together and placed in 23 mL PTFE lined acid digestion vessels. The reaction was conducted at 100 °C for 18 h. The product was rinsed with methanol and water before activation at 150 °C.

UIO-66. The previously reported synthesis method[16] was implemented as follows: $ZrCl_4$ (0.636 g, 2.73 mmol) and terephthalic acid (TPA) (0.453 g, 2.73 mmol) were dissolved via stirring in 106 mL of DMF. The solution was divided up equally and placed in ten 20 mL scintillation vials. The vials were placed in a sand bath at 120 °C and reacted for 20 h. The resultant product was rinsed with DMF three times before activation at 200 °C. The amino version of UiO-66 was synthesized following the same procedure, substituting terephthalic acid with amino-terephthalic acid (ATPA).

dx.doi.org/10.1021/ie202325p | Ind. Eng. Chem. Res. 2012, 51, 6513−6519

DMOF-1. The procedure reported by Wang et al.[5] was used to solvothermally synthesize DMOF-1. $Zn(NO_3)_2{\cdot}6H_2O$ (1.74 g, 6.00 mmol), TPA (1.02 g, 6.00 mmol), and 1,4-diazabicyclo[2.2.2]octane or DABCO (1.08 g, 9.63 mmol) were dissolved in 150 mL of DMF. The solution was then filtered three times to remove the white precipitate and placed in ten 20 mL scintillation vials in a sand bath. The sand bath was heated from 35 to 120 °C at a rate of 2.5 °C/min and reacted for 12 h. The product was rinsed with DMF three times and activated at 110 °C.

DMOF-1-NH$_2$. Again, the procedure reported by Wang et al.[5] was used to solvothermally synthesize DMOF-1-NH_2. $Zn(NO_3)_2{\cdot}6H_2O$ (1.79 g, 6.02 mmol), ATPA (1.10 g, 6.09 mmol), and DABCO (1.08 g, 9.63 mmol) were dissolved in 150 mL of DMF. The solution was then filtered three times to remove the white precipitate and placed in fifteen 20 mL scintillation vials in a sand bath. The sand bath was heated from 35 to 120 °C at a rate of 2.5 °C/min, and the vials were allowed to react for 12 h. The product was rinsed with DMF three times and then placed in a Sohxlet extractor for solvent exchange with chloroform for 72 h at 90 °C.

2.2. Adsorption Isotherm Measurement. Water adsorption isotherms were measured at 298 K and 1 bar on an IGA-003 microbalance from Hiden Isochema. All MOF samples were activated in situ to remove residual solvent and water adsorbed during sample loading, which requires brief exposure (c.a. 3 min) to ambient air. Dry air was used as the carrier gas, with a portion of the carrier gas being bubbled through a vessel of deionized water. The relative humidity (RH) was controlled by varying the ratio of saturated air and dry air via two mass flow controllers. Experiments were conducted up to 90% RH due to water condensation in the apparatus at higher humidities. The total gas flow rate was 200 cm^3/min for the entire experiment. Variable timeouts were used with a maximum limit of 24 h per isotherm point. Due to fluctuating climate control of the laboratory itself, condensation inside the gravimetric adsorption apparatus can occur at 90% RH. In this case, equilibrium was not reached due to continued mass gain from condensation, and desorption data were not reported. After the isotherms were collected, the samples were regenerated under dynamic vacuum and elevated temperature. Reactivation temperatures for each MOF are given in the Supporting Information (Table S1).

2.3. Characterization. Powder X-ray diffractograms are collected using a PANalytical X-ray diffractometer. Initial sample sizes for each material are on the order of 200 mg and are able to fill a bulk XRD sample holder. However, due to size limitations of the gravimetric adsorption sample pan, reactivated samples are on the order of 50 mg. Diffractograms are collected under ambient conditions, and humidity exposure is minimized via storage in sealed vials. Nitrogen adsorption isotherms at 77 K were measured for each MOF before and after water exposure using a Quadrasorb system from Quantachrome Instruments.

3. RESULTS AND DISCUSSION

Figure 1 shows water adsorption and desorption isotherms for HKUST-1 and Mg MOF-74 at 298 K. As expected, both open metal site materials exhibit a strong affinity for water, with loadings of 33 and 37 mol/kg for HKUST-1 and Mg MOF-74, respectively, at ~90% RH. These results are consistent with previous reports that open-metal site MOFs have high affinities for small molecules containing accessible lone pairs of electrons

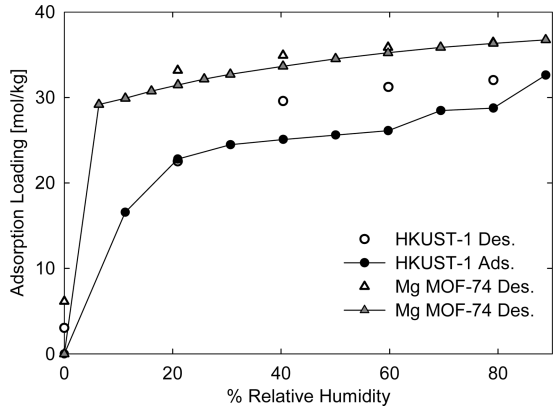

Figure 1. Water adsorption and desorption isotherms for open metal site MOFs, HKUST-1 and Mg MOF-74, at 298 K and 1 bar.

such as CO_2 and H_2O.[3,19,33,34,38] In agreement with the findings of Kaskel et al.,[19] the hysteresis curves show that a portion of the water cannot be desorbed under flowing dry air. At 0% relative humidity, Mg MOF-74 retains more water than HKUST-1 upon desorption; Mg MOF-74 retains 17% of maximum uptake compared to 9% retained by HKUST-1.

Water adsorption plots for UiO-66, DMOF-1, and the amine-functionalized analogues are shown in Figure 2. Of these

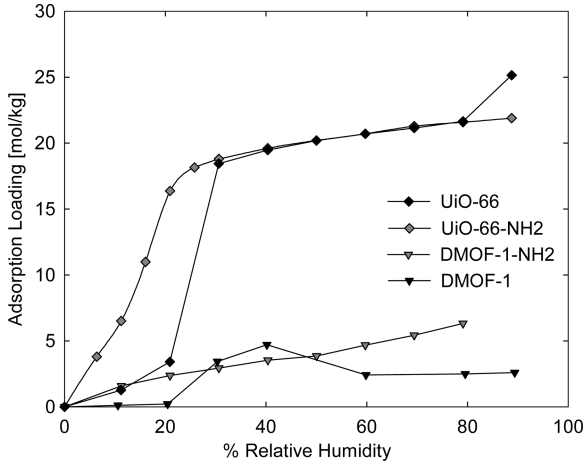

Figure 2. Water adsorption isotherms for parent materials, UiO-66 and DMOF-1, along with their amine-functionalized analogues, UiO-66-NH_2 and DMOF-1-NH_2, at 298 K and 1 bar.

four MOFs, the zirconium based UiO-66 and amine-functionalized analogue exhibit the highest water uptake at humidity levels greater than or equal to 30% RH. UiO-66 adsorbs relatively little water below 20% RH but then exhibits a sharp step in the isotherm in which adsorption loadings increase from 3 to 16 mmol/g. This MOF has been reported to undergo a transition from the as-synthesized 8-coordinated state to 7-coordinated upon dehydroxylation.[16] The observed step in the isotherm may correspond to a transition back to the 8-coordinated state, but the step is more likely attributed to pore filling also reported by Llewellyn et al.[32] This point will be revisited in later discussion. The desorption isotherms of UiO-66 and UiO-6-NH_2 (Supporting Information Figure S9 and S10) exhibit hysteresis indicative of the inability to remove a portion of the water under flowing dry air. At 0% RH, UiO-66 and UiO-66-NH_2 retain 1.7 and 2.8 mmol H_2O/g, respectively,

dx.doi.org/10.1021/ie202325p | Ind. Eng. Chem. Res. 2012, 51, 6513–6519

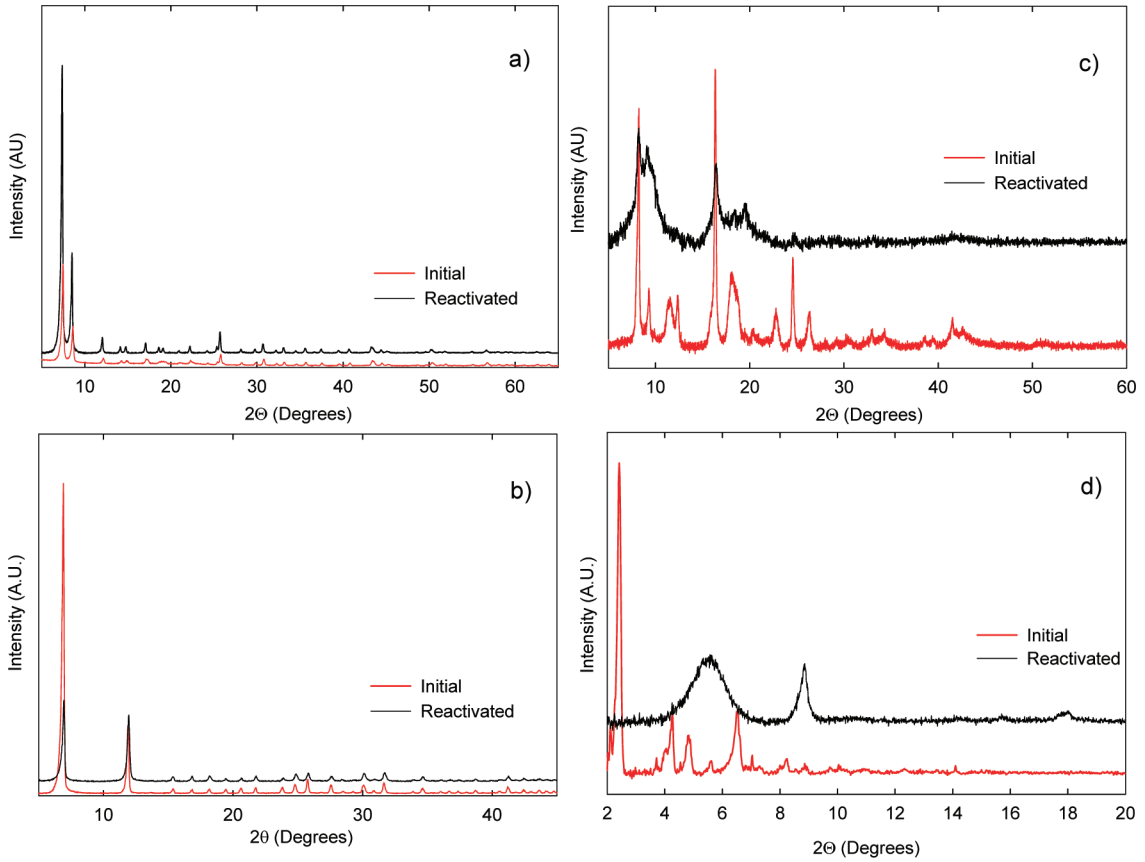

Figure 3. PXRD results for (a) UiO-66-NH_2, (b) Mg-MOF-74, (c) DMOF-1-NH_2, and (d) UMCM-1.

which suggests rehydroxylation of the samples during water adsorption and is in agreement with the reported results from Llewellyn and co-workers.[32] For UiO-66-NH_2, the adsorption isotherm exhibits more rectangular or Type I behavior below 20% RH compared to the parent material, which along with the increased water retention under dry air flow are indicative of the preferred amine−water interactions. In agreement with what others have reported,[28,38,41] we find that DMOF-1 displays the most hydrophobic character of all the materials in this study up to 20% RH. Above this concentration, we see atypical adsorption behavior in agreement with the findings of Liang et al.[38] More specifically, a sharp increase in uptake at 30% RH followed by a decrease from 40 to 60% RH. In this case, the loss of adsorbed water despite increasing water vapor concentration is likely an attribute of both the structure loss of the adsorbent itself and the hydrophobic properties of the degradation product, DABCO. DMOF-1-NH_2 exhibits an increase in water adsorption compared to the hydrophobic parent material and does not demonstrate the same loss of adsorbed water. This is likely due to the hydrophilic character of the proposed degradation product, ATPA.

The compilation of adsorption isotherms is shown in Supporting Information Figure S6. For the zinc-carboxylate MOF, UMCM-1, the adsorption isotherm nearly mirrors DMOF-1-NH_2 adsorption until 40% RH, but at higher humidity levels there is a more rapid increase in uptake. From a pore volume perspective (2.41 cm^2/g), the low uptake results for UMCM-1 are surprising.

To examine the possible degradation of the tested materials, powder XRD data were collected for the as-synthesized samples and for the samples exposed to humid conditions and reactivated. Figure 3 illustrates the apparent structure retention of UiO-66-NH_2 and Mg-MOF-74 and the significant loss of crystallinity for DMOF-1-NH_2 and UMCM-1. UiO-66 and HKUST-1 also retained their crystallinity based on PXRD (Supporting Information), but it is important to note that slight degradation of the structure may not show up in the powder X-ray patterns due to high intensities of the peaks at low angles. The hydrolysis degradation reaction appears to describe the UMCM-1 structure loss; at higher values of 2Θ, there is evidence of $Zn(OH)_2$, which is a direct product of this reaction.[21] The degradation of UMCM-1 is not surprising considering that the coordination environment is identical to MOF-5, which is well-known to decompose under humid conditions. The significant loss of crystallinity in the DMOF-1 materials is somewhat surprising considering the hydrophobic nature of the parent material under low relative humidity and the relatively high pK_a of the DABCO ligand. However, the zinc-carboxylate coordination is notoriously unstable and likely the weakest link which initiates the framework collapse, in spite of the Zn−N coordination from the DABCO ligand.

Further support of the stability analysis is captured by BET surface area analysis of the initial and reactivated samples. These results are shown in Table 1. The water uptake at 80% RH for each MOF does not directly correlate with pore volume or diameter. Instead, site preferences and degradation dictate the water adsorption. For example, the open-metal site materials with relatively small pore volumes, HKUST-1 and Mg MOF-74, show significantly higher uptake than UMCM-1. This is due to the open-metal site MOFs' affinity for water and also due to the degradation of UMCM-1. Similarly, DMOF-1 and DMOF-1-NH_2 have significantly lower water loadings of

dx.doi.org/10.1021/ie202325p | Ind. Eng. Chem. Res. 2012, 51, 6513−6519

Table 1. Adsorption Loadings at 80% Relative Humidity and BET Surface Area Comparison of Samples before Water Exposure and after Isotherm Measurement and Reactivation

material	pore volume[b] (cm^2/g)	pore diameter (Å)	loading, 80% RH[c] (cm^3/g)	surface area (m^2/g) before	surface area (m^2/g) after	% loss
Mg-MOF-74[a]	0.65	11	0.62	1400	238	83
UiO-66-NH_2	0.57	<6	0.37	1040	1050	0
UiO-66	0.52	~6	0.37	1160	1130	2
DMOF-1	0.58	7.5 × 7.5; 4.8 × 3.2	0.04	1960	7	100
DMOF-1-NH_2	0.58	7.5 × 7.5; <4.8 × 3.2	0.11	2010	0	100
HKUST-1[a]	0.62	9; 6	0.49	1270	945	26
UMCM-1	2.41	27 × 32; 14 × 17	0.11	6010	205	97

[a]Contains open metal sites. [b]Obtained from the Dubinin–Astakov model of N_2 adsorption at 77 K. [c]Condensation effects observed at higher humidity levels.

0.04 and 0.11 cm^3/g at 80% RH, respectively compared to their accessible pore volumes of 0.58 cm^3/g from N_2 adsorption at 77 K. This is attributed to the degradation of DMOF-1 and DMOF-1-NH_2 throughout the water isotherm collection, which is in agreement with the PXRD data (Figure 4 and Supporting Information Figure S1). The increased water uptake exhibited by the amine-functionalized version is likely due to the hydrophilic character of the ATPA ligand itself. In agreement with PXRD results, UiO-66 and the amine-functionalized analogue display negligible loss of surface area. Water loadings of 0.37 cm^3/g at 80% RH for both UiO-66 and UiO-66-NH_2 match well with the value previously reported.[32] Nevertheless, these water uptakes are less than pore volumes obtained via N_2 adsorption. This is likely an attribute of the rehydroxylation of the materials during water exposure. BET modeling of the N_2 adsorption at 77 K for UMCM-1 confirm the degradation apparent in the XRD analysis, showing almost total loss in surface area. Despite structure confirmation via XRD, both of the open metal site MOFs undergo significant reduction in surface area. HKUST-1 and Mg MOF-74 show 26 and 83% loss, respectively. Kaskel et al.[19] also report a significant loss in BET surface area, 48%, for HKUST-1 following water adsorption and reactivation. The Dietzel group show the complete stability of MOF-74 materials during cyclic dehydration/rehydration experiments under inert atmosphere,[22,24] but Ni MOF-74 was shown to degrade during identical testing in the presence of oxygen.[23] The dehydration or reactivation procedure of our study utilized dynamic vacuum, which may have prevented oxygen exposure from contributing to structure degradation. However, since air was used as a carrier gas, the entrained oxygen in the adsorbed water appears to sufficiently supply the degradation reaction during reactivation. However, this could not be determined conclusively from the available data.

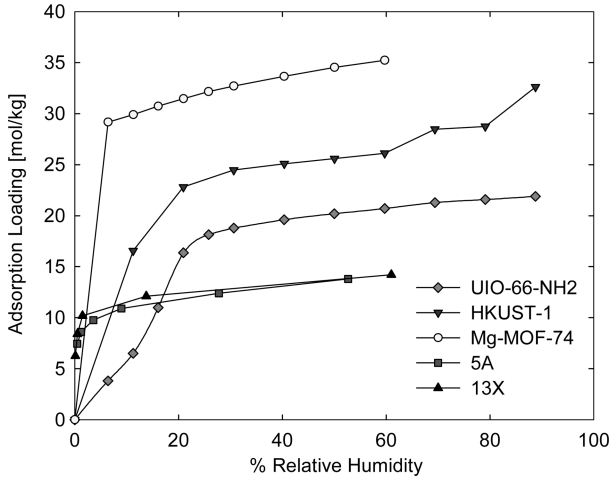

Figure 4. Water adsorption isotherms for UiO-66-NH_2, HKUST-1, and Mg MOF-74 compared with zeolites 5A and 13X from the work of Wang et al.,[37] all at 298 K.

Greater insight into water adsorption behavior of MOFs can be gained by comparing our results with adsorption in traditional porous materials. Adsorption isotherms for UiO-66-NH_2, Mg-MOF-74, and HKUST-1 are compared in Figure 4 with water adsorption in zeolites[42] 5A and 13X. The calcium and sodium cations in 5A and 13X, respectively, provide strong adsorption sites for water at low relative pressure. The more rectangular Type I isotherms are indicative of this behavior. The MOFs with open-metal sites show analogous hydrophilicity but have much higher saturation loadings compared to the zeolites due to larger pore volumes. The rectangular Type I isotherm for UiO-66-NH_2 compared to the parent material (Figure 2) illustrates the favorable impact of amino functional groups on water adsorption.

A comparison of water isotherms for UiO-66 and DMOF-1 with BPL carbon[43] and mesoporous silicas[44] MCM-41 and SBA-1 is shown in Figure 5. These materials exhibit Type V isotherms, which are characteristic of strong fluid–fluid interactions. The pore filling occurs first for UiO-66, which has pore sizes of ca. 6 Å and is immediately followed by DMOF-1, with 7.5 Å and 4.5 × 3.8 Å pores. SBA-1 (21 Å pores) undergoes condensation at the next lowest pressure, followed by BPL carbon, which possesses a distribution of pore

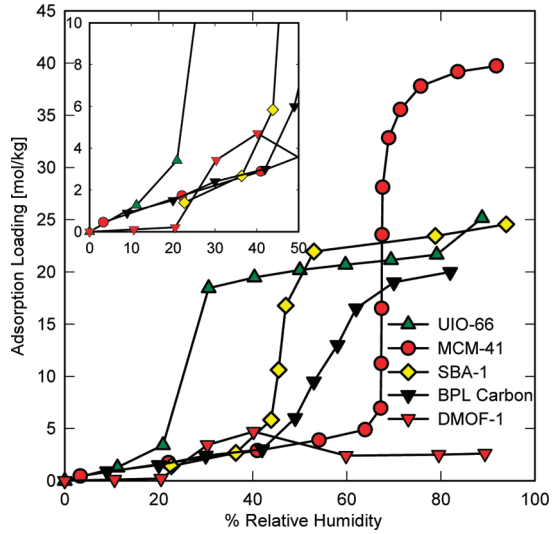

Figure 5. Water adsorption isotherms for UiO-66 (298 K) compared with MCM-41 (293 K), SBA-1 (293 K), and BPL carbon (298 K).

dx.doi.org/10.1021/ie202325p | Ind. Eng. Chem. Res. 2012, 51, 6513–6519

sizes (6−18 Å). The pore filling step occurs last for the largest-pore material (30 Å) MCM-41. It is difficult to decouple the effects of pore size, local functionalization, and wetting on the adsorption behavior. However, in the absence of highly favorable adsorption sites (e.g., cations, open-metal sites, or oxygenated sites), adsorption of water within a porous structure will occur primarily through pore filling. This condensation arises due to the overlapping potential of the pore walls and will be dictated by the size of the pore. Thus, pore filling, or the step in the isotherm, will occur at the lowest relative pressure of water for the material with the smallest pores. For materials with no local functionalization of the pore space, water will have stronger interactions within the bulk liquid state than with the surface. Because of this, condensation will not occur until the bulk pressure is higher than the saturation vapor pressure (i.e., $P/P_0 > 1$).[45,46] On the other hand, local functionalization or heterogeneity of the surface will lead to adsorption of water at lower pressures. The adsorbed water molecules then provide stable hydrogen-bonding networks within the pores, which consequently lead to adsorption saturation below P_0.[45,46]

Mesoporous silicas and activated carbons typically have some degree of local functionalization in the form of silanol groups, carbonyls, etc. UiO-66 has no analogous functionalization, but the small pore size and metal oxide cluster most likely contribute to apparent pore filling at 20% RH. The desorption isotherm of UiO-66 (Supporting Information Figure S8) exhibits low pressure hysteresis that is similar to the H1 classification, which indicates the presence of micropores.[47] DMOF-1 possesses micropores with diameters similar to UiO-66 and exhibits pore filling at nearly the same point, ca. 20% RH. However, the indicative water adsorption step is less significant in DMOF-1, and the desorption data are not capable of confirming complete pore filling due to the complete framework collapse which occurs during the water adsorption above 40% RH.

4. CONCLUSION

In summary, we have performed an investigation of water vapor adsorption and subsequent structural analysis of a representative set of metal−organic frameworks. The crystal structure of UMCM-1 was completely degraded after water exposure and regeneration. This instability is attributed to the four-coordinated zinc-carboxylate system. The amine-functionalized and parent forms of DMOF-1 also exhibited a complete loss of crystallinity after water exposure at 90% RH. Both the parent and functionalized UiO-66 show good structural stability via complete PXRD peak agreement and negligible BET surface area loss. This is attributed to the higher stability of the Zr inorganic cluster. The adsorption behavior of UiO-66 and DMOF-1 are analogous to pore filling in heterogeneous pore spaces of mesoporous silicas and carbons. MOFs with open-metal sites strongly bind water and exhibit isotherm shapes similar to zeolites 5A and 13X. These MOFs are difficult to regenerate after water exposure by heating under vacuum. PXRD patterns suggest that the crystalline structures are retained to some extent, but BET surface areas of the materials decreased substantially and are indicative of some structure loss during the adsorption-reactivation process likely due to the use of dry air as the carrier gas. Oxygen exposure itself or the presence of entrained oxygen in the adsorbed water phase may facilitate the degradation. This work provides a systematic investigation of water adsorption in prototypical MOFs and shows that in some cases these materials display water adsorption behavior that is comparable to conventional adsorbents such as zeolites and activated carbon. Nevertheless, additional studies of water adsorption in MOFs for a wide range of metals and ligands are necessary to truly develop design criteria for synthesizing water-stable materials.

■ ASSOCIATED CONTENT

Supporting Information

Activation/regeneration conditions, powder XRD comparisons, and full water adsorption/desorption isotherms. This material is available free of charge via the Internet at http://pubs.acs.org.

■ AUTHOR INFORMATION

Corresponding Author

*E-mail: krista.walton@chbe.gatech.edu.

Notes

The authors declare no competing financial interest.

■ ACKNOWLEDGMENTS

This material is based upon work supported by Army Research Office PECASE Award W911NF-10-0079 and Contract W911NF-10-0076.

■ REFERENCES

(1) Ferey, G. Some Suggested Perspectives for Multifunctional Hybrid Porous Solids. *Dalton Trans.* **2009**, 4400.

(2) Kuppler, R. J.; Timmons, D. J.; Fang, Q. R.; Li, J. R.; Makal, T. A.; Young, M. D.; Yuan, D. Q.; Zhao, D.; Zhuang, W. J.; Zhou, H. C. Potential Applications of Metal-Organic Frameworks. *Coord. Chem. Rev.* **2009**, *253*, 3042.

(3) Caskey, S. R.; Wong-Foy, A. G.; Matzger, A. J. Dramatic Tuning of Carbon Dioxide Uptake via Metal Substitution in a Coordination Polymer with Cylindrical Pores. *J. Am. Chem. Soc.* **2008**, *130*, 10870.

(4) Rowsell, J. L. C.; Yaghi, O. M. Effects of Functionalization, Catenation, and Variation of the Metal Oxide and Organic Linking Units on the Low-Pressure Hydrogen Adsorption Properties of Metal-Organic Frameworks. *J. Am. Chem. Soc.* **2006**, *128*, 1304.

(5) Wang, Z. Q.; Tanabe, K. K.; Cohen, S. M. Tuning Hydrogen Sorption Properties of Metal-Organic Frameworks by Postsynthetic Covalent Modification. *Chem.—Eur. J.* **2010**, *16*, 212.

(6) Farha, O. K.; Hupp, J. T. Rational Design, Synthesis, Purification, and Activation of Metal-Organic Framework Materials. *Acc. Chem. Res.* **2010**, *43*, 1166.

(7) Tanabe, K. K.; Cohen, S. M. Postsynthetic Modification of Metal-Organic Frameworks-a Progress Report. *Chem. Soc. Rev.* **2011**, *40*, 498.

(8) Li, J. R.; Kuppler, R. J.; Zhou, H. C. Selective Gas Adsorption and Separation in Metal-Organic Frameworks. *Chem. Soc. Rev.* **2009**, *38*, 1477.

(9) Huang, L. M.; Wang, H. T.; Chen, J. X.; Wang, Z. B.; Sun, J. Y.; Zhao, D. Y.; Yan, Y. S. Synthesis, Morphology Control, and Properties of Porous Metal-Organic Coordination Polymers. *Microporous Mesoporous Mat.* **2003**, *58*, 105.

(10) Greathouse, J. A.; Allendorf, M. D. The Interaction of Water with MOF-5 Simulated by Molecular Dynamics. *J. Am. Chem. Soc.* **2006**, *128*, 10678.

(11) Kaye, S. S.; Dailly, A.; Yaghi, O. M.; Long, J. R. Impact of Preparation and Handling on the Hydrogen Storage Properties of Zn4O(1,4-benzenedicarboxylate)(3) (MOF-5). *J. Am. Chem. Soc.* **2007**, *129*, 14176.

(12) Wu, T. J.; Shen, L. J.; Luebbers, M.; Hu, C. H.; Chen, Q. M.; Ni, Z.; Masel, R. I. Enhancing the Stability of Metal-Organic Frameworks in Humid Air by Incorporating Water Repellent Functional Groups. *Chem. Commun.* **2010**, *46*, 6120.

(13) Hausdorf, S.; Wagler, J.; Mossig, R.; Mertens, F. Proton and Water Activity-Controlled Structure Formation in Zinc Carboxylate-Based Metal Organic Frameworks. *J. Phys. Chem. A* **2008**, *112*, 7567.

(14) Choi, H. J.; Dinca, M.; Dailly, A.; Long, J. R. Hydrogen Storage in Water-Stable Metal-Organic Frameworks Incorporating 1,3-and 1,4-benzenedipyrazolate. *Energy Environ. Sci.* **2010**, *3*, 117.
(15) Park, K. S.; Ni, Z.; Cote, A. P.; Choi, J. Y.; Huang, R. D.; Uribe-Romo, F. J.; Chae, H. K.; O'Keeffe, M.; Yaghi, O. M. Exceptional Chemical and Thermal Stability of Zeolitic Imidazolate Frameworks. *Proc. Natl. Acad. Sci. U. S. A.* **2006**, *103*, 10186.
(16) Cavka, J. H.; Jakobsen, S.; Olsbye, U.; Guillou, N.; Lamberti, C.; Bordiga, S.; Lillerud, K. P. A New Zirconium Inorganic Building Brick Forming Metal Organic Frameworks with Exceptional Stability. *J. Am. Chem. Soc.* **2008**, *130*, 13850.
(17) Ehrenmann, J.; Henninger, S. K.; Janiak, C. Water Adsorption Characteristics of MIL-101 for Heat-Transformation Applications of MOFs. *Eur. J. Inorg. Chem.* **2011**, 471.
(18) Akiyama, G.; Matsuda, R.; Kitagawa, S. Highly Porous and Stable Coordination Polymers as Water Sorption Materials. *Chem. Lett.* **2010**, *39*, 360.
(19) Kusgens, P.; Rose, M.; Senkovska, I.; Frode, H.; Henschel, A.; Siegle, S.; Kaskel, S. Characterization of Metal-Organic Frameworks by Water Adsorption. *Microporous Mesoporous Mat.* **2009**, *120*, 325.
(20) Cychosz, K. A.; Matzger, A. J. Water Stability of Microporous Coordination Polymers and the Adsorption of Pharmaceuticals from Water. *Langmuir* **2010**, *26*, 17198.
(21) Low, J. J.; Benin, A. I.; Jakubczak, P.; Abrahamian, J. F.; Faheem, S. A.; Willis, R. R. Virtual High Throughput Screening Confirmed Experimentally: Porous Coordination Polymer Hydration. *J. Am. Chem. Soc.* **2009**, *131*, 15834.
(22) Dietzel, P. D. C.; Morita, Y.; Blom, R; Fjellvag, H. An In Situ High-Temperature Single-Crystal Investigation of a Dehydrated Metal-Organic Framework Compound and Field-Induced Magnetization of One-Dimensional Metal-Oxide Chains. *Angew. Chem., Int. Ed.* **2005**, *44*, 6354−6358.
(23) Dietzel, P. D. C.; Panella, B.; Hirscher, M.; Blom, R.; Fjellvag, H. Hydrogen Adsorption in a Nickel Based Coordination Polymer with Open Metal Sites in the Cylindrical Cavities of the Desolvated Framework. *Chem. Commun.* **2006**, 959−961.
(24) Dietzel, P. D. C.; Blom, R.; Fjellvag, H. Base-Induced Formation of Two Magnesium Metal-Organic Framework Compounds with a Bifunctional Tetratopic Ligand. *Eur. J. Inorg. Chem.* **2008**, 3624−3632.
(25) Chui, S. S. Y.; Lo, S. M. F.; Charmant, J. P. H; Orpen, A. G.; Williams, I. D. A Chemically Functionalizable Nanoporous Material Cu-3(TMA)(2)(H2O)(3) (n). *Science* **1999**, *283*, 1148.
(26) Rosi, N. L.; Kim, J.; Eddaoudi, M.; Chen, B. L.; O'Keeffe, M.; Yaghi, O. M. Rod Packings and Metal-Organic Frameworks Constructed from Rod-Shaped Secondary Building Units. *J. Am. Chem. Soc.* **2005**, *127*, 1504.
(27) Garibay, S. J.; Cohen, S. M. Isoreticular Synthesis and Modification of Frameworks with the UiO-66 Topology. *Chem. Commun.* **2010**, *46*, 7700.
(28) Lee, J. Y.; Olson, D. H.; Pan, L.; Emge, T. J.; Li, J. Microporous Metal-Organic Frameworks with High Gas Sorption and Separation Capacity. *Adv. Funct. Mater.* **2007**, *17*, 1255.
(29) Koh, K.; Wong-Foy, A. G.; Matzger, A. J. A Crystalline Mesoporous Coordination Copolymer with High Microporosity. *Angew. Chem., Int. Ed.* **2008**, *47*, 677.
(30) Zlotea, C.; Phanon, D.; Mazaj, M.; Heurtaux, D.; Guillerm, V.; Serre, C.; Horcajada, P.; Devic, T.; Magnier, E.; Cuevas, F.; Ferey, G.; Llewellyn, P. L.; Latroche, M. Effect of NH(2) and CF(3) functionalization on the hydrogen sorption properties of MOFs. *Dalton Trans.* **2011**, *40*, 4879.
(31) Valenzano, L.; Civalleri, B.; Chavan, S.; Bordiga, S.; Nilsen, M. H.; Jakobsen, S.; Lillerud, K. P.; Lamberti, C. Disclosing the Complex Structure of UiO-66 Metal Organic Framework: A Synergic Combination of Experiment and Theory. *Chem. Mater.* **2011**, *23* (7), 1700−1718.
(32) Wiersum, A. D.; Soubeyrand-Lenoir, E.; Yang, Q. Y.; Moulin, B.; Guillerm, V.; Ben Yahia, M.; Bourrely, S.; Vimon, A.; Miller, S.; Vagner, C.; Daturi, M.; Clet, G.; Serre, C.; Maurin, G.; Llewellyn, P. L. An Evaluation of UiO-66 for Gas-Based Applications. *Chem.—Asian J.* **2011**, *6* (12), 3270−3280.
(33) Keskin, S.; van Heest, T. M.; Sholl, D. S. Can Metal-Organic Framework Materials Play a Useful Role in Large-Scale Carbon Dioxide Separations? *ChemSusChem* **2010**, *3*, 879.
(34) Liu, J.; Wang, Y.; Benin, A. I.; Jakubczak, P.; Willis, R. R.; LeVan, M. D. CO2/H2O Adsorption Equilibrium and Rates on Metal-Organic Frameworks: HKUST-1 and Ni/DOBDC. *Langmuir* **2010**, *26*, 14301.
(35) Millward, A. R.; Yaghi, O. M. Metal-Organic Frameworks with Exceptionally High Capacity for Storage of Carbon Dioxide at Room Temperature. *J. Am. Chem. Soc.* **2005**, *127*, 17998.
(36) Wang, Q. M.; Shen, D. M.; Bulow, M.; Lau, M. L.; Deng, S. G.; Fitch, F. R.; Lemcoff, N. O.; Semanscin, J. Metallo-Organic Molecular Sieve for Gas Separation and Purification. *Microporous Mesoporous Mat.* **2002**, *55*, 217.
(37) Glover, T. G.; Peterson, G. W.; Schindler, B. J.; Britt, D.; Yaghi, O. MOF-74 Building Unit Has a Direct Impact on Toxic Gas Adsorption. *Chem. Eng. Sci.* **2011**, *66*, 163.
(38) Liang, Z. J.; Marshall, M.; Chaffee, A. L. CO2 Adsorption, Selectivity and Water Tolerance of Pillared-Layer Metal Organic Frameworks. *Microporous Mesoporous Mat.* **2010**, *132*, 305.
(39) Wang, Z. Q.; Tanabe, K. K.; Cohen, S. M. Accessing Postsynthetic Modification in a Series of Metal-Organic Frameworks and the Influence of Framework Topology on Reactivity. *Inorg. Chem.* **2009**, *48*, 296.
(40) Mu, B.; Schoenecker, P. M.; Walton, K. S. Gas Adsorption Study on Mesoporous Metal-Organic Framework UMCM-1. *J. Phys. Chem. C* **2010**, *114*, 6464.
(41) Chen, Y. F.; Lee, J. Y.; Babarao, R.; Li, J.; Jiang, J. W. A Highly Hydrophobic Metal Organic Framework Zn(BDC)(TED)(0.5) for Adsorption and Separation of CH3OH/H2O and CO2/CH4: An Integrated Experimental and Simulation Study. *J. Phys. Chem. C* **2010**, *114*, 6602.
(42) Wang, Y.; Levan, M. D. Adsorption Equilibrium of Carbon Dioxide and Water Vapor on Zeolites 5A and 13X and Silica Gel: Pure Components. *J. Chem. Eng. Data* **2009**, *54*, 2839.
(43) Rudisill, E. N.; Hacskaylo, J. J.; Levan, M. D. Coadsorption of Hydrocarbons and Water on BPL Activated Carbon. *Ind. Eng. Chem. Res.* **1992**, *31*, 1122.
(44) Oh, J. S.; Shim, W. G.; Lee, J. W.; Kim, J. H.; Moon, H.; Seo, G. Adsorption Equilibrium of Water Vapor on Mesoporous Materials. *J. Chem. Eng. Data* **2003**, *48*, 1458.
(45) Liu, J. C.; Monson, P. A. Does Water Condense in Carbon Pores? *Langmuir* **2005**, *21*, 10219.
(46) Monson, P. A. Contact Angles, Pore Condensation, and Hysteresis: Insights from a Simple Molecular Model. *Langmuir* **2008**, *24*, 12295.
(47) Sing, K. S. W.; Everett, D. H.; Haul, R. A. W.; Moscou, L.; Pierotti, R. A.; Rouquerol, J.; Siemieniewska, T. Reporting Physisorption Data for Gas Solid Systems with Special Reference to the Determination of Surface-Area and Porosity (Recommendations 1984). *Pure Appl. Chem.* **1985**, *57*, 603.